

Semiclassical Dynamics Simulation of the Photodissociation of Cyclobutane

Yusheng Dou^{a,b,*}, Yibo Lei^{a,c}, Anyang Li^a, Ben R. Torralva^d, Glenn V. Lo^b, and Roland E. Allen^e

^a Bio-Informatics Institute, Chongqing University of Posts and Telecommunications, Chongqing, 400065, P. R. China

^b Department of Physical Sciences, Nicholls State University, PO Box 2022, Thibodaux, LA 70310, U. S. A.

^c Modern Physical Institute, Northwest University, Xi'an, 710069, P. R. China

^d Chemistry and Materials Science, Lawrence Livermore National Laboratory, Livermore, CA 94550, U. S. A.

^e Department of Physics, Texas A&M University, College Station, Texas 77843, U. S. A.

Abstract

Semiclassical electron-radiation-ion dynamics simulations are reported for the photodissociation of cyclobutane into two molecules of ethylene. The results clearly show the formation of the tetramethylene intermediate diradical, with dissociation completed in roughly 400 femtoseconds. In addition, the potential energy surfaces of the electronic ground state and lowest excited state were calculated at the CASSCF/MYPT2 level with 6-31G* basis sets, along the reaction path determined by the SERID simulations. There are well-defined energy minima and maxima in the intermediate state region. It is found that both C-C-C bond bending and rotation of the molecule (around the central C-C bond) play important roles in determining the features of the potential energy surfaces for the intermediate species. Finally, the simulations and potential energy surface calculations are employed together in a discussion of the full mechanism for cyclobutane photodissociation.

*^y Electronic email: Yusheng.Dou@nicholls.edu

I. Introduction

The dissociation of cyclobutane to form two molecules of ethylene (or the reverse process) is a textbook example of an addition/elimination reaction involving the Woodward-Hoffmann rules¹, and it has been well studied both experimentally and theoretically². Two different mechanisms were originally proposed: In the first picture, the reaction proceeds directly through a transition state at the saddle point of the activation barrier. In the second, it proceeds through a two-step process, with one of the C-C bonds first breaking to form tetramethylene, a diradical reaction intermediate, which then passes through a transition state, finally yielding two molecules of ethylene.

Thermodynamic analysis of appropriately substituted precursors³⁻⁷, as well as of the cycloaddition of ethylene to form butane⁸, suggested the existence of the diradical intermediate. Development of techniques based on ultrashort laser pulses finally made it possible to directly study the dynamics of the intermediates in chemical reactions: Using femtosecond laser techniques, together with time-of-flight mass spectrometry in a molecular beam, Zewail and coworkers identified the reactive immediate, the tetramethylene diradical, in the transition state on a real time scale^{9,10}. In their experiments, the diradicals are produced by the decarbonation of cyclopentanone initiated by a femtosecond-scale laser pulse. It has been found that the tetramethylene diradical immediately decays, at 340, 700, or 840 fs depending on the total energy used.

A large number of quantum calculations at different levels have been performed¹¹⁻²¹ to locate the minimum and saddle points of the potential energy surface for the electronic ground state of tetramethylene. Various calculations have yielded somewhat controversial results

regarding the existence of energy wells near the transition state of the reaction. Calculations at the CASSCF level suggest^{13,14} that there are two minima and six saddle points on the potential energy surface of tetramethylene. Computations at a higher level, for example with the MR-AQCC approximation, indicate²¹ that these stationary points and their relative energies are significantly dependent on the level of theory employed. It should be noted that the stationary points studied in these investigations are mainly along a reaction path involving only rotation of the diradical about the central C-C bond or dissociation of the second C-C bond. Few of them include terminal CH₂ twist motion²¹.

Here we report studies which employ both (i) semiclassical electron-radiation-ion dynamics (SERID), a technique for simulations of the electronic and nuclear dynamics following an applied laser pulse^{22,23}, and (ii) calculations of the potential energy surfaces for the electronic ground state and lowest excited state at the CASSCF/MYPT2 level with 6-31G* basis sets. We will first discuss our SERID simulations of the ring opening reaction of cyclobutane to form two molecules of ethylene. The results of these simulations provide a microscopic picture of the formation of the tetramethylene diradical immediate and detailed information on its dynamics. We will then consider the potential energy surfaces, following the reaction path from reactant to product as determined by the simulation. The electronic ground state potential energy surface is found to show rather well-defined energy wells. The potential energy surfaces calculated in this way involve all the nuclear degrees of freedom, and allow us to investigate how the reaction pathway, particularly near the transition state, is affected by different internal coordinates.

II. Methodology

In our semiclassical electron-radiation-ion dynamics approach, the time-dependent quantum states are calculated for the valence electrons, but both the radiation field and the motion of the nuclei are treated classically. As one can see from time-dependent perturbation theory, such a semiclassical treatment includes effective “ n -photon” and “ n -phonon” processes in absorption and stimulated emission. This fact permits us to examine nontrivial processes such as multi-electron and multi-photon excitations, the indirect excitation of vibrational modes, intra-molecular vibrational energy redistribution, and interdependence of the various electronic and vibrational degrees of freedom.

A detailed description of this method has been published elsewhere^{22,23}, so only a brief outline is given here. The one-electron states are updated at each time step by solving the time-dependent Schrödinger equation in a nonorthogonal basis,

$$i\hbar \frac{\partial \psi_j}{\partial t} = \mathbf{S}^{-1} \cdot \mathbf{H} \cdot \psi_j, \quad 1$$

where \mathbf{S} is the overlap matrix for the atomic orbitals. The electrons are coupled to the vector potential \mathbf{A} of the radiation field through the time-dependent Peierls substitution²⁴

$$H_{ab}(\mathbf{X} - \mathbf{X}') = H_{ab}^0(\mathbf{X} - \mathbf{X}') \exp\left(\frac{iq}{\hbar c} \mathbf{A} \cdot (\mathbf{X} - \mathbf{X}')\right). \quad (2)$$

Here $H_{ab}(\mathbf{X} - \mathbf{X}')$ is the Hamiltonian matrix element for basis functions a and b on atoms with position vectors \mathbf{X} and \mathbf{X}' respectively, and $q = -e$ is the charge of the electron.

The Hamiltonian matrix, overlap matrix, and effective nuclear-nuclear repulsion are based on density-functional calculations.²⁵ In our previous investigations of C_{60} responding to laser pulses of various intensities²⁶, and of the photocyclization of cis-stilbene to

dihydrophenanthrene²⁷, this same model was found to yield a very good description of C-C bond cleavage and closure.

The nuclear motion is determined by the Ehrenfest equation of motion

$$M_l \frac{d^2 X_{l\alpha}}{dt^2} = - \sum_j \psi_j^\dagger \cdot \left(\frac{\partial \mathbf{H}}{\partial X_{l\alpha}} - i\hbar \frac{\partial \mathbf{S}}{\partial X_{l\alpha}} \frac{\partial}{\partial t} \right) \cdot \psi_j - \frac{\partial U_{rep}}{\partial X_{l\alpha}} \quad (3)$$

where U_{rep} is the effective nuclear-nuclear repulsive potential.

The time-dependent Schrödinger equation (1) is solved using a unitary algorithm which is based on the equation for the time evolution operator²⁸. Equation (3) is numerically integrated with the velocity Verlet algorithm (which preserves phase space). A time step of 50 attoseconds was used, since this yielded satisfactory energy conservation.

As indicated in Fig. 1 (a), all nuclear degrees of freedom are included in the calculation. Before the cyclobutane molecule is coupled to the vector potential, it is given a puckered geometry and allowed 1000 fs to relax to its optimized ground state geometry at a temperature of 300 K. The laser pulse was taken to have a full-width-at-half-maximum (FWHM) duration of 100 fs (with a profile which is very nearly Gaussian²⁸) a fluence of 0.90 kJ/m², and a wavelength corresponding to a photon energy of 6.50 eV. This wavelength matches the density-functional energy gap between the HOMO and LUMO levels of cyclobutane.²⁹ The fluence was chosen such that the forces on the nuclei are large enough to break two nonadjacent C-C bonds successively, but not to break any C-H bond. Simulations with slightly different initial conditions do not exhibit significantly different results from those presented here.

The potential energy surfaces of both the electronic ground state and the first excited state were calculated at the CASSCF/MRPT2 level with 6-31G* basis sets, using the XIAN CI

cod³⁰ with no symmetry restriction, and with 4 electrons and 4 orbitals included in the active space. For tetramethylene, there are then states of the same symmetry and spin multiplicity, and we broke the degeneracy by including states outside the active space, labeled by β . First the energies and corresponding eigenvectors were obtained in standard CASSCF calculations:

$$\mathbf{E}_0^i, \Psi_0^i = \sum_{R \in \text{CAS}} \mathbf{C}_R^i \Phi_R \quad (i=1, 2, \dots). \quad (4)$$

Then Rayleigh-Schrödinger perturbation theory was used to obtain the nondegenerate energies using an iterative procedure:

$$\mathbf{E}^i = \mathbf{E}_0^i + \sum_{\beta \notin \text{CAS}} \frac{|\langle \Psi_0^i | \mathbf{H} | \Phi_\beta \rangle|^2}{\mathbf{E}_0^i - \mathbf{E}_\beta} \quad (5)$$

where the \mathbf{E}_β are the energies calculated in the previous iteration.

III. Results and Discussion

Four snapshots from the simulation at different times are shown in Fig. 1. About 190 fs after the beginning of the laser pulse (which has a full duration of 200 fs), the C₁-C₃ bond is broken and the tetramethylene intermediate is formed. Then, at about 365 fs, the C₂-C₄ bond is broken and two ethylene molecules are produced. The lifetime of the tetramethylene intermediate can be defined as the time until the second C-C bond is broken, and the value found in the simulation is thus comparable to the experimental value of 340 fs. After 450 fs, the two ethylenes move away each other.

The variation of the C₁-C₂ bond with time is shown in Fig. 2. It is clear that this is a single bond in cyclobutane, and that it becomes a double bond in ethylene: Starting at about 0.155 nm, the length of a typical C-C single bond, the C₁-C₂ bond vibrates strongly after the laser pulse is applied. After 190 fs, its length decreases, but is still longer than 0.135 nm, the length of a regular C-C double bond, because the diradical has formed. After 365 fs, with the

dissociation into two ethylene molecules, this C₁-C₂ bond is finally shortened to about 0.135 nm, and it remains at this length until the end of the simulation.

The variations with time of the C₁-C₃ and C₂-C₄ distances are shown in Fig. 3. It is clear that the C₁-C₃ bond breaks just before 200 fs and the C₂-C₄ bond dissociates not long after 350 fs. The variation of the C₁-C₃ distance between 200 and 350 fs exhibits dynamical features of the tetramethylene intermediate diradical associated with variations of the C₁-C₂-C₄-C₃ torsional angle and the C-C-C angles.

Figure 4 shows the time dependence of both the C₁-C₂-C₄-C₃ and the H₃-C₂-C₄-H₇ torsional angles. Neither varies significantly before about 200 fs, when the tetramethylene intermediate diradical is formed. Starting from 0°, the diradical rotates about the C₂-C₄ bond during the next 100 fs to about -100°, and then turns back. It passes through 0° at about 365 fs and continues trivially to increase after the C₂-C₄ bond is broken. The time dependence of the C₁-C₂-C₄ and C₃-C₄-C₂ angles are shown in Fig. 5. Between 190 and 365 fs, one can see large-amplitude angle-bending vibrations which result from breaking of the C₁-C₃ bond to form the diradical.

Figure 6 shows the variations with time of the H₁-C₁-C₂-H₄ torsional angle, which rotates from -180° to 0°, with vibrations, while in the diradical configuration.

The variations with time of the HOMO and LUMO energies are presented in Fig. 7, and the time-dependent population of the LUMO in Fig. 8. (It should be mentioned that the HOMO and HOMO-1 of the cyclobutane ultimately evolve into two identical HOMOs of the ethylene molecules after dissociation, and the original LUMO and LUMO+1 similarly evolve into two identical LUMOs.) Figure 7 demonstrates the abrupt change in the HOMO and

LUMO energies when the C₁-C₃ bond breaks, at about 190 fs. There are two close approaches of these levels, with avoided crossings, with the energy separations being 0.111 eV at 197.6 fs and 0.106 eV at 250.4 fs. The coupling of the states at 197.6 fs produces only weak electronic transitions, as can be seen in Fig. 8. On the other hand, the coupling at 250.4 fs results in the rather dramatic nonadiabatic transitions from LUMO to HOMO that can also be observed in Fig. 8.

In order to understand the dissociation process more completely, we have performed completely independent calculations of the total energy for both the ground state and the first excited state of the molecule, as a function of time, along the reaction path determined in the SERID simulation described above. These calculations were performed at the CASSCF/MRPT2 level with 6-31G* basis sets, and the results are shown in Fig. 9. (It should be emphasized that the curves of Fig. 9 are one-dimensional “potential energy surfaces”, corresponding to the classical nuclear trajectories determined “on the fly” in a simulation, for which the electron-radiation-ion dynamics is given by Eqs. (1)-(3).) The results clearly indicate a reaction intermediate state, between roughly 200 and 450 fs. There are two rather well-defined energy wells in the ground state PES, one at about 330 fs, labeled A, and another at about 410 fs, labeled B. It can be seen from Figs. 5 and 9 that the electronic ground state PES is largely determined by variations in the C-C-C angles: The two energy wells are associated with C-C-C angles near 90° (the initial value in cyclobutane), while the higher energy regions I, II, and III are associated with C-C-C angles substantially different from 90°. Figures 4 and 9 clearly show that the large deviation of the C₁-C₂-C₄-C₃ torsional angle from its initial value of 0° is also associated with the intermediate state of the molecule. We conclude that the C-C-C

angles and the $C_1-C_2-C_4-C_3$ torsional angle are the main internal reaction coordinates that define the features of the ground state potential energy surface in the intermediate state region. Expansion of the C-C-C angle appears to increase the ground state energy, while the rotation of the molecule about the C_2-C_4 bond (away from 0°) lowers it. The same is true of the first excited state, whose behavior is also shown in Fig. 9.

IV. Conclusions

The combination of SERID simulations and CASSCF calculations of the potential energy surfaces (for the ground state and lowest excited state of the molecule while “on the fly”) provides a clear picture of the mechanism for photodissociation of cyclobutane to form two molecules of ethylene: When a femtosecond-scale laser pulse is applied, there is a HOMO to LUMO excitation during the first 200 fs, and one C-C bond breaks to form the intermediate tetramethylene diradical, which then moves on its lowest excited-state potential energy surface. At about 240 fs, the diradical decays to its electronic ground state, because of electronic transitions induced by nonadiabatic coupling between the LUMO and HOMO. The diradical subsequently moves on its ground-state potential energy, with rotation about the central C-C bond. Cleavage of the second C-C bond – i.e. dissociation into two ethylene molecules – occurs at roughly 400 fs in our simulations. We find that the C-C-C-C torsional angle is an important internal coordinate during the reaction, but C-C-C bond bending also plays a key role in shaping the potential energy surface for the tetramethylene intermediate.

Acknowledgements

The authors acknowledge support by the American Chemical Society Petroleum Research Fund (Grant 45446-B6), the Research Fund of Chongqing University of Posts and Telecommunications, China (Grant A2006-81), the National Natural Science Foundation of China (Grant 200473060), and the Robert A. Welch Foundation (Grant A-0929). The Supercomputer Facility at Texas A&M University provided computational assistance.

REFERENCES

1. R. Woodward and R. B. Hoffmann, *The Conservation of Orbital Symmetry* (Academic, New York, 1970).
2. J. Berson, *Science* **266**, 1338 (1994), and references therein.
3. H. R. Gerberich and W. D. Walters, *J. Am. Chem. Soc.* **83**, 3935 (1961).
4. H. R. Gerberich and W. D. Walters, *J. Am. Chem. Soc.* **83**, 4884 (1961).
5. P. B. Dervan and T. Uyehara, *J. Am. Chem. Soc.* **98**, 1262 (1976).
6. P. B. Dervan and T. Uyehara, *J. Am. Chem. Soc.* **101**, 2076 (1979).
7. P. B. Dervan, T. Uyehara, and D.S. Santilli, *J. Am. Chem. Soc.* **102**, 3863 (1980).
8. G. Scacchi, C. Richard, and M. H. Back, *Int. J. Chem. Kinet.* **9**, 513 (1977).
9. S. Pedersen, J. L. Herek, and A. H. Zewail, *Science* **266**, 1359 (1994).
10. J.C. Polanyi and A. H. Zewail, *Acc. Che. Res.* **28**, 119 (1995).
11. W. T. Borden and E. R. Davidson, *J. Am. Chem. Soc.* **102**, 5409 (1980).
12. F. Bernardi, A. Bottoni, M. A. Robb, H. B. Schlegel, and G. Tonachini, *J. Am. Chem. Soc.* **107**, 2260 (1985).
13. F. Bernardi, A. Bottoni, P. Celani, M. Olivucci, M. A. Robb, and A. Venturini, *Chem. Phys. Lett.* **192**, 229 (1992).
14. C. Doubleday, *J. Am. Chem. Soc.* **115**, 11968 (1993).
15. C. Doubleday, *Chem. Phys. Lett.* **233**, 509 (1995).
16. C. Doubleday, *J. Phys. Chem.* **100**, 15083 (1996).
17. C. Doubleday, K. Bolton, G. H. Peslherbe, and W. L. Hase, *J. Am. Chem. Soc.* **118**, 9922 (1996).

18. N. W. Moriarty, R. Lindh, and G. Karlström, *Chem. Phys. Lett.* **289**, 442 (1998).
19. K. N. Houk, B. R. Reno, M. Nendel, K. Black, H. Young Yoo, S. Wilsey, and J. K. Lee, J. *Mol. Struct.: THEOCHEM* **398–399**, 169 (1997).
20. S. De Feyter, E. W. G. Diau, A. A. Scala, and A. H. Zewail, *Chem. Phys. Lett.* **303**, 249 (1999).
21. E. Ventura, M. Dallos, and H. Lischka, *J. Chem. Phys.* **118**, 10963 (2003).
22. Y. Dou, B. R. Torralva, and R. E. Allen, *J. Mod. Optics* **50**, 2615 (2003).
23. Y. Dou, B. R. Torralva, and R. E. Allen, *Chem. Phys. Lett.* **378**, 323 (1998).
24. T. B. Boykin, R. C. Bowen, and G. Klimeck, *Phys. Rev. B* **63**, 245314 (2001).
25. D. Porezag, Th. Frauenheim, Th. Köhler, D. Seifert, and R. Kaschner, *Phys. Rev. B* **51**, 12947 (1995).
26. B. R. Torralva, T. A. Niehaus, M. Elstner, S. Suhai, Th. Frauenheim, and R. E. Allen, *Phys. Rev. B* **64**, 153105 (2001).
27. Y. Dou, and R. E. Allen, *J. Mod. Optics* **51**, 2485 (2004).
28. R. E. Allen, T. Dumitrica, and B. R. Torralva, in *Ultrafast Physical Processes in Semiconductors*; Tsen, K. T., Eds. (Academic Press, New York, 2001), Chapter 7.
29. The experimental energy gap between HOMO and LUMO is () eV. As usual, density-functional calculations yield a lower value for the gap.
30. Y. Wang, B. Suo, G. Zhai, and Z. Wen, *Chem. Phys. Lett.* **389**, 315 (2004).

FIGURE CAPTIONS

FIG. 1. Snapshots from semiclassical dynamics simulation of the photodissociation of cyclobutane to form two ethylene molecules. Note that the first C-C bond is broken at about 190 fs, and the second at about 365 fs. An animation file for this reaction is available at http://www.nicholls.edu/phsc/ydou/ring_opening_cyclobutane.htm .

FIG. 2. Time dependence of a C-C bond ultimately associated with one ethylene molecule. Notice that this bond begins to shorten in the intermediate state, and becomes a double bond after dissociation.

FIG. 3. Time dependence of the C₁-C₃ and C₂-C₄ bonds. One can observe both the sequence of bond-breaking and the dynamics of the tetramethylene diradical intermediate.

FIG. 4. Changes in the dihedral angles C₁-C₂-C₃-C₄ and H₄-C₂-C₄-H₇ in tetramethylene. After about 400 fs, the C₂-C₄ bond has been broken and the behavior of these angles is no longer physically meaningful.

FIG. 5. Variation with time of the C₁-C₂-C₄ and C₂-C₄-C₃ bond bending angles.

FIG. 6. Changes in the dihedral angle H₁-C₁-C₂-H₄.

FIG. 7. Variation with time of the HOMO and LUMO levels.

FIG. 8. Time-dependent population of the LUMO.

FIG. 9. Potential energy surfaces (as defined in the text) for the electronic ground state and lowest excited state of the molecule, calculated at the CASSCF/MRPT2 level with 6-31G* basis sets. The nuclear positions in the molecule at each time step were determined in the semiclassical dynamics simulation described in text.

FIG. 1.

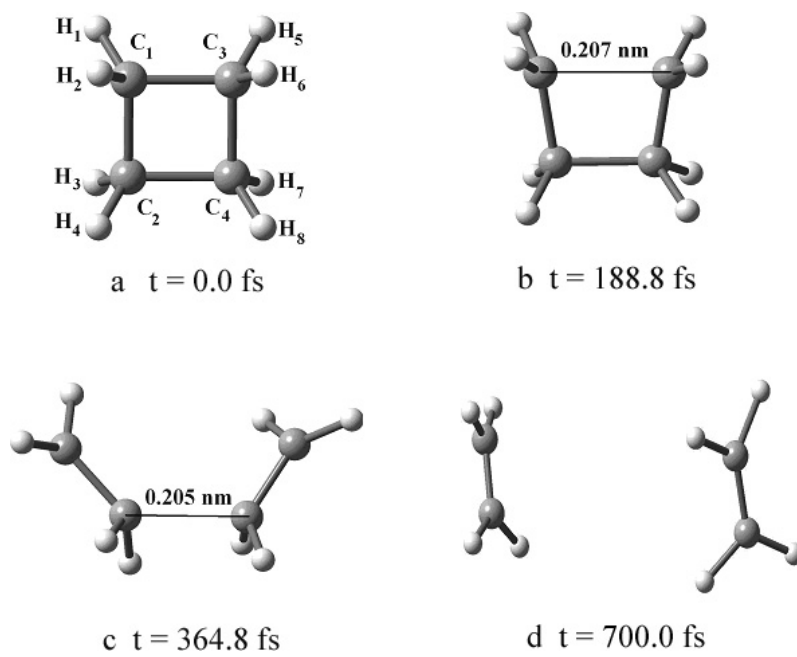


FIG. 2.

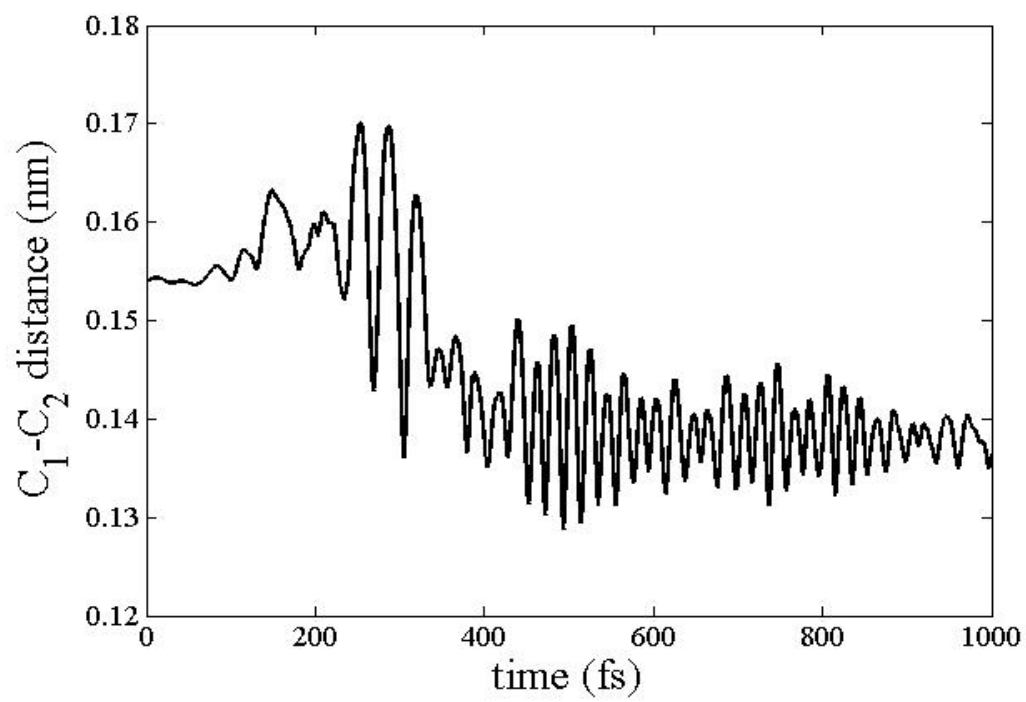


FIG. 3.

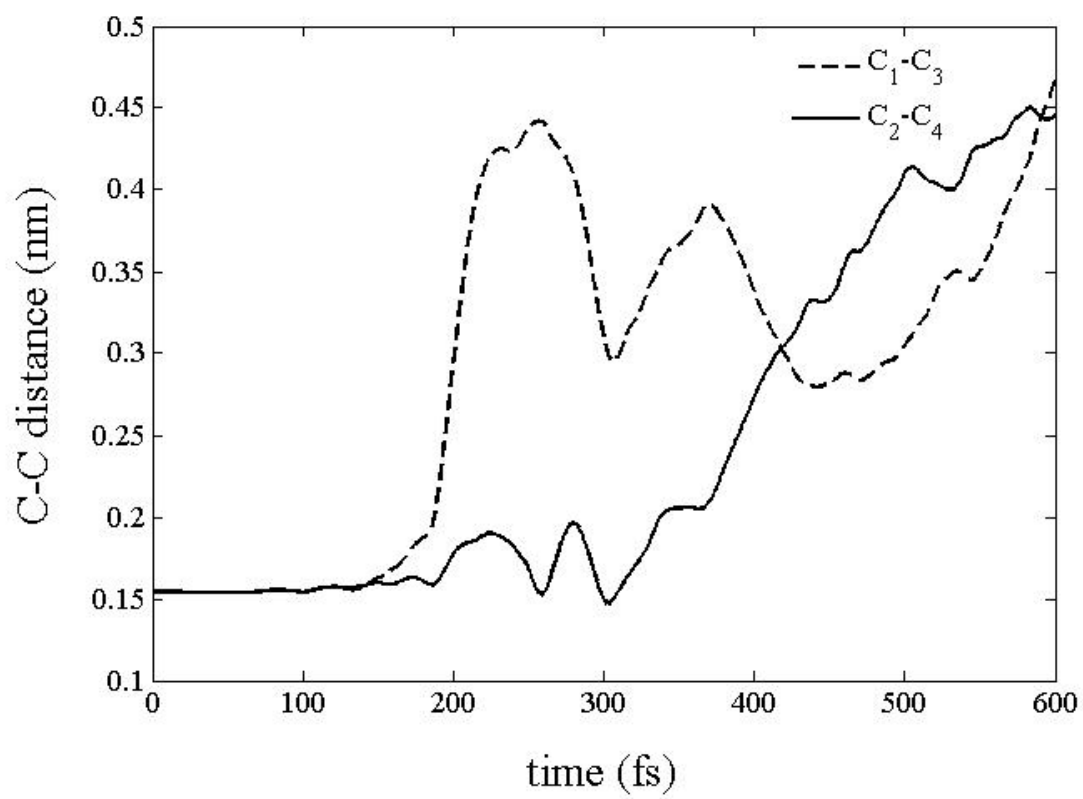


FIG. 4.

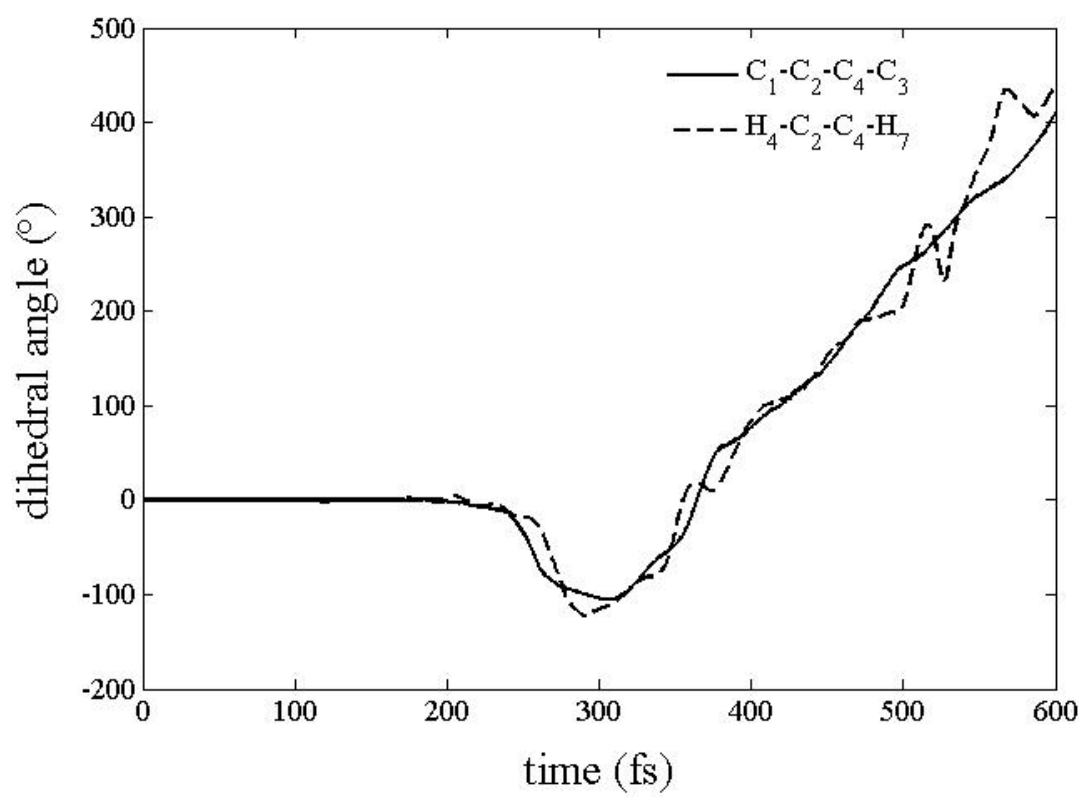


FIG. 5.

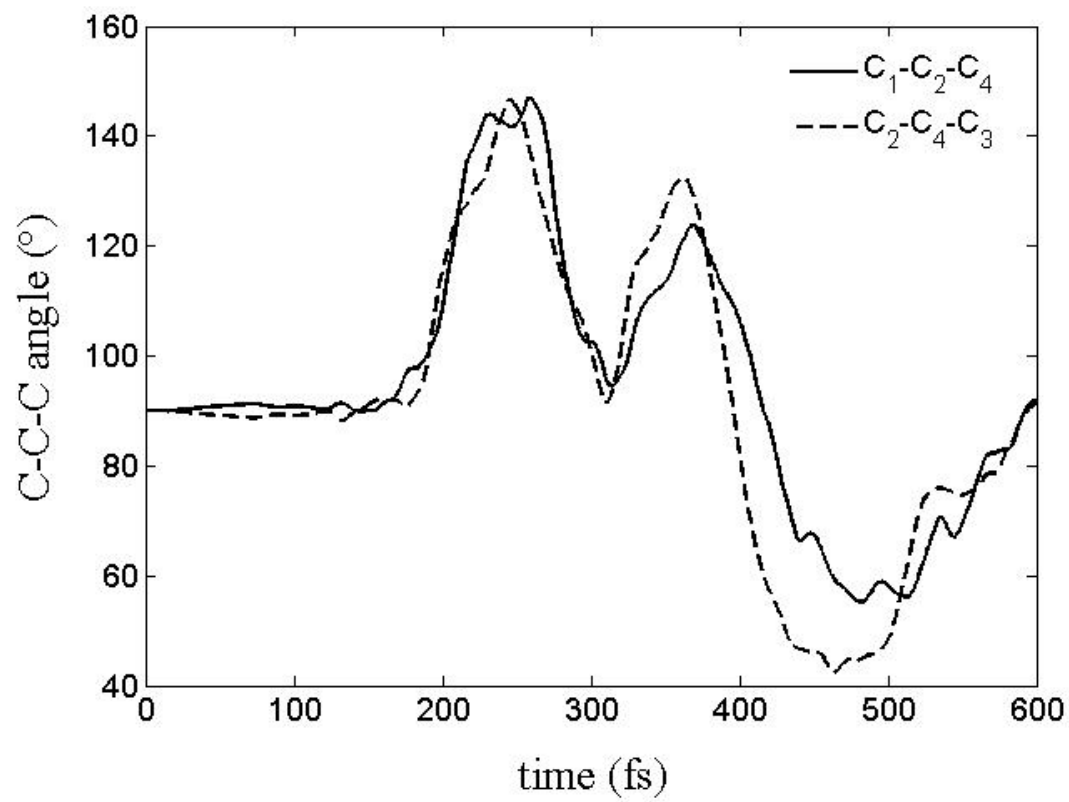


FIG. 6.

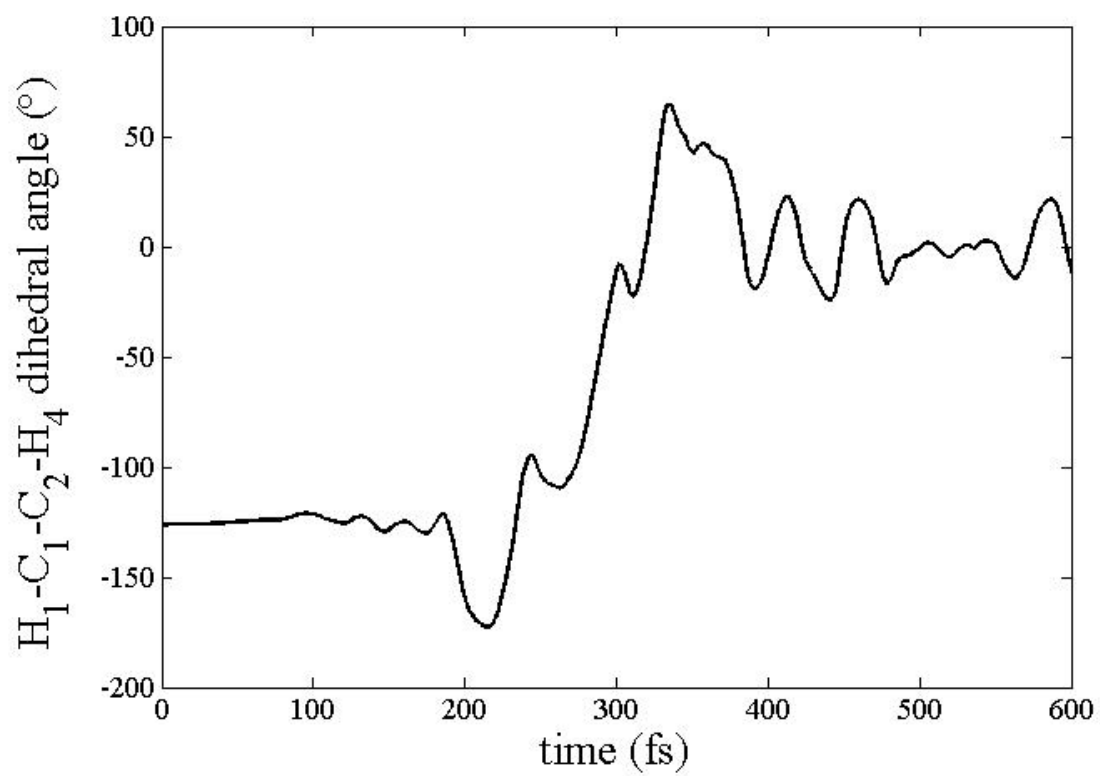


FIG. 7.

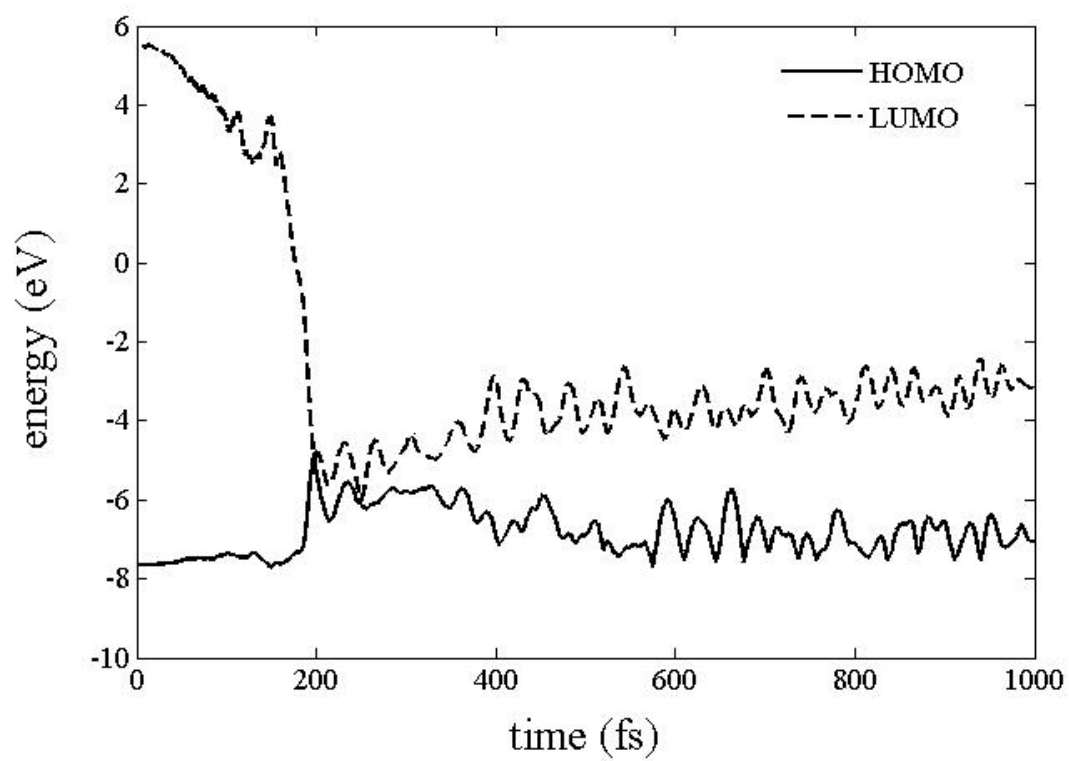


FIG. 8.

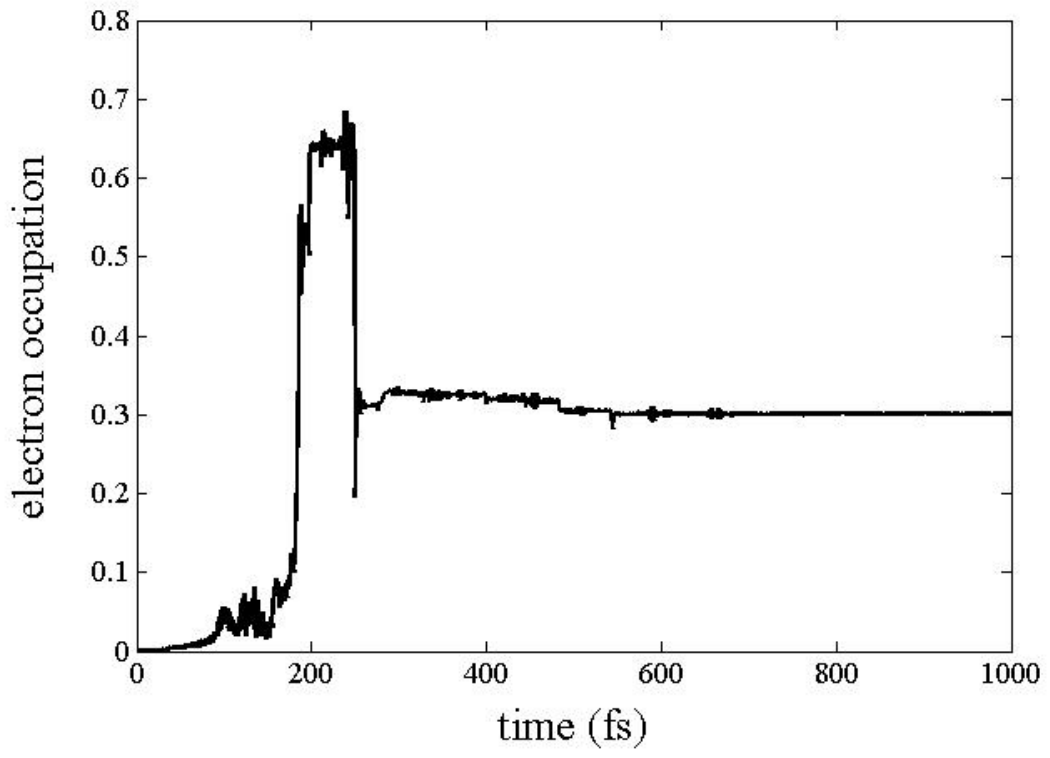


FIG. 9.

